Aidah Abd Al-Doori
Awatif S. Jasim

Department of Physics,
College of Science,
Tikrit University,
Tikrit, IRAQ

High-Performance NO_2 Gas Sensor Based on ZnO:SnO_2 Nanoparticles Prepared by Pulsed-Laser Deposition

Thin films of ZnO nanoparticle-doped SnO_2 by 30% and 50% were prepared on glass substrates by pulsed-laser deposition (PLD). The structural examinations of the prepared samples showed that the XRD patterns demonstrate a polycrystalline structure, with the grain size decreasing with increasing SnO_2 doping ratio. The elemental composition of ZnO doped with varying SnO_2 doping ratios was determined by EDX analysis, which revealed that the film is composed of Zn, Sn, and O_2, with the ratios varying according to the doping ratio. The optical properties show that the samples are characterized by high absorption in the ultraviolet spectrum, while the band gap values decreased with increasing the ratios of doping of SnO_2 from 3.22 eV to 3.05 eV. The sensor results showed a very high response to NO_2 gas for all ratios and at different temperatures. This response increased with an increase in the doped ratio of SnO_2, reaching 1344.40% at 100°C, with a response time of 20.7 s.

Keywords: Tin dioxide; Pulsed-laser deposition; NO_2 gas; Gas sensors
Received: 27 March 2025; **Revised:** 12 May 2025; **Accepted:** 194 May 2025

1. Introduction

Air pollution is one of the problems that pose a threat to the natural environment. As a result of the rapid development in the world, numerous toxic gases are released daily in significant amounts, such as nitrogen compounds, carbides, sulfides, and volatile organic compounds, which negatively affects human health [1]. NO_2, one of the primary air pollutants that contributes to a number of illnesses, the most important of which are respiratory illnesses [2]. So, gas detection is of great importance for maintaining health and protecting the environment. Gas sensors are essential for many uses, such as detecting poisoning from gas in indoor places and monitoring factory gas explosions [3-5].

Recently, many researchers have been interested in nanoscale semiconductors due to their important role in solving many basic physical issues and their future uses as innovative materials [6-8]. Semiconductors with wide energy gaps (3.37 and 3.6 eV), such as ZnO and SnO_2, are significant oxides that are frequently employed in general or gas sensor applications, so researchers have focused on this type of oxide [9-11]. Because nanoscale SnO_2 is inexpensive, it has garnered a lot of interest. [12], gas-sensitive properties [13], and good electrical and thermal conductivity. However, pure nanoscale SnO_2 materials lack high sensor response and selectivity. In order to enhance gas sensors' ability to detect gases, numerous researchers have attempted to dope with other elements in order to produce defects (like oxygen vacancies). [14]. To increase the sensitivity, responsiveness, and gas selectivity, several additional oxides have been used, including CdO, WO_3, CeO_2, and ZnO [15,16]. In this study, zinc oxide (ZnO) was used, which is a transparent conducting oxide with high infrared reflectivity and high transmittance in the spectrum's visible region [17] It was doped with tin oxide in different proportions to make a gas sensor for NO_2 gas at different temperatures.

High-resolution films can be made using PLD technology at low temperatures. It is described as the process of a material entering a vacuum system under a specific pressure and vaporizing, and a tiny quantity of the material that forms the plasma column can be vaporized or ablated by the laser energy intensity at each pulse. [18]. It is a method that is used to prepare films in this study.

2. Experimental Part

In this research, the PLD method was used at a pressure of 10^{-3} mbar, with a wavelength of 1064 nm, and a frequency of 6 Hz to prepare films of pure ZnO and doped with ratios of 50% and 30% of tin oxide. They were ground and mixed using a ceramic grinder and then pressed using a hydraulic press under a pressure of 5 tons for 5 min to create a target weighing 2 g. Then, the films were prepared on a clean substrate from glass with a thickness of 1 mm and dimensions of 26×76 mm^2, positioned 3 cm away from the target and exposed to a 400-pulse laser beam, and the films were annealed at 450°C for 2 hours. Following an analysis of the prepared films' optical and structural characteristics, a gas sensor was manufactured by depositing aluminum masks in the form of individual clips on the prepared films using the thermal evaporation system as shown in Fig. (1), and the sensor's sensitivity to NO_2 gas at various temperatures was then examined.

Fig. (1) The mask pattern of gas sensor

3. Results and Discussion

Figure (2) shows the XRD patterns of ZnO doped films at various SnO_2 atomic ratios. The XRD patterns show polycrystalline hexagonal structure for prepared films, corresponded to the standard card (00-036-1451) for ZnO. Crystallization was enhanced by increasing the tin content to 50%, where the added material acted as a catalyst for crystal growth [19]. Additional peaks emerged at ZnO50%:$SnO_2$50% film that matched SnO_2 crystals arranged at 61.98°, which were attributed to the (310) crystal plane of tin oxide with the standard card (00- 029- 1484). As a result of changes in the applied stress on the lattice, the width of the peaks changed due to the change in particle size [20]. The grain size decreased as a result of increasing the percentage of SnO_2 to 50%, as shown in table (1).

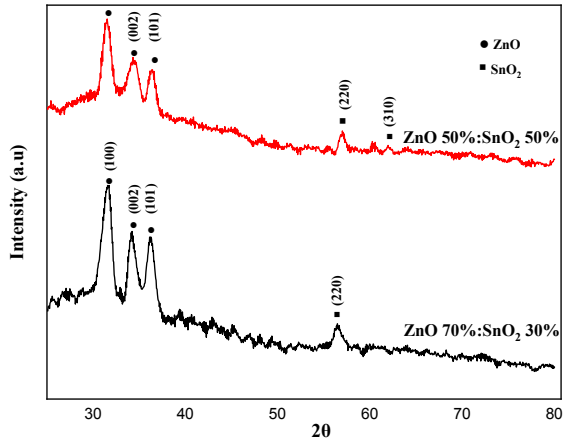

Fig. (2) XRD patterns for the ZnO:SnO_2 thin films prepared at different ratios

AFM was used to study film surface topography and roughness. Figure (3) shows AFM pictures of ZnO70%:$SnO_2$30% and ZnO50%:$SnO_2$50% thin films. The analysis shows that all films have a flat surface with no cracks or pinholes and are found to be homogeneous with nanometer-sized roughness [21], and it showed that the grain size of prepared films decreased as a result of increasing the SnO_2 ratio. This result is in good agreement with [22], while roughness and the RMS increased as a result of increasing the SnO_2 ratio to 50%, as shown in table (2). That is, the doping ratio has a clear effect on the surface topography of the prepared films [23].

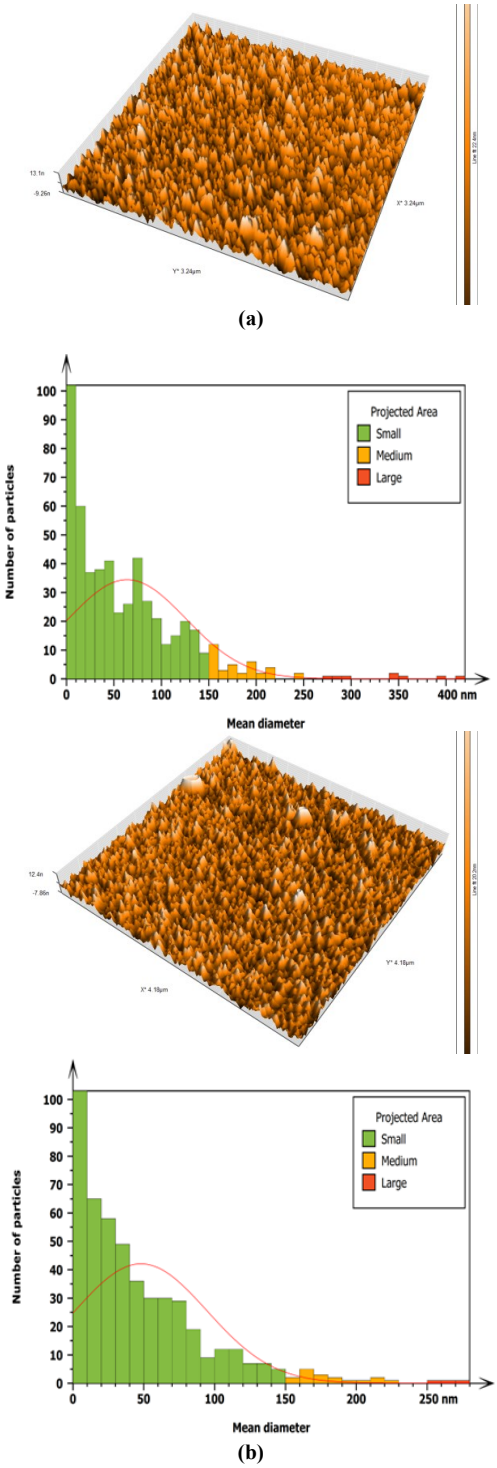

Fig. (3) AFM images for (a) ZnO 70%:SnO_2 30% and (b) ZnO 50%:SnO_2 50%

Figure (4) shows SEM results of the samples prepared to determine the morphology, forms, and sizes of the nanoparticles. The images show that in the ZnO70%:$SnO_2$30% sample, the particle size increases

to about 26.20 nm, with some particles clumping together into large groups. This is a generally observed phenomenon of reduced surface energy [24]. But when the ratio of SnO_2 increases in the ZnO50%:$SnO_2$50% sample, we notice a decrease in the size of the particles and their regular spherical arrangement, and this is mainly for the gas sensor. All images show the high density of the structures and the similarity of the shapes with their repetition. This structure may be attributed to the penetration of tin oxide atoms into the crystal lattice of zinc oxide and thus worked to slightly change its crystal levels, which led to the compression of some hexagonal crystals and the preservation of others.

Table (2) AFM Parameters for ZnO:SnO_2 thin film

Samples	T(°C)	Response time (s)	Recovery time (s)	Sensitivity (%)
ZnO 70%: SnO_2 30%	100	25.2	62.1	29.56
	150	22.5	67.5	559.18
	200	24.3	45.9	247.06
ZnO 50%: SnO_2 50%	100	20.7	67.5	1344.40
	150	25.2	46.8	1049.56
	200	0	0	0

Figure (5) shows EDX analysis confirmed that the thin films consist of elements (Zn), (Sn), and (O). Adding to that, we observe that the Au element is present in analysis results; gold is applied to the surface because it needs to be clean and flat for the analysis process. The results showed that the decrease in the percentage of nanoparticles (Zn) and the increase in the oxygen ratio when the doping ratio increases is a result of the material clumping in a specific area. The reason for this is the difference in the atomic sizes of the two materials [25].

As for the optical properties, the absorption occurs in the range of about 350 nm, the films are characterized by high absorption in the ultraviolet region, and it can be noted that increasing the ratio of doping of SnO_2 to 50% led to an increase in optical absorption as shown in Fig. (6). This is explained by the fact that impurities in the energy gap close to the conduction band cause donor levels to emerge, leading to a shift in the absorption edge towards long wavelengths [26]. The band gap value decreased from 3.22 eV to 3.05 eV with increasing the ratios of doping of SnO_2, as shown in Fig. (7). As mentioned above, Impurities have caused donor levels to form within the energy gap close to the conduction band, which is why the energy gap has decreased. These levels are prepared to receive electrons and generate tails in the optical energy gap. These tails work to decreasing the gap and thus will absorb low-energy photons [27].

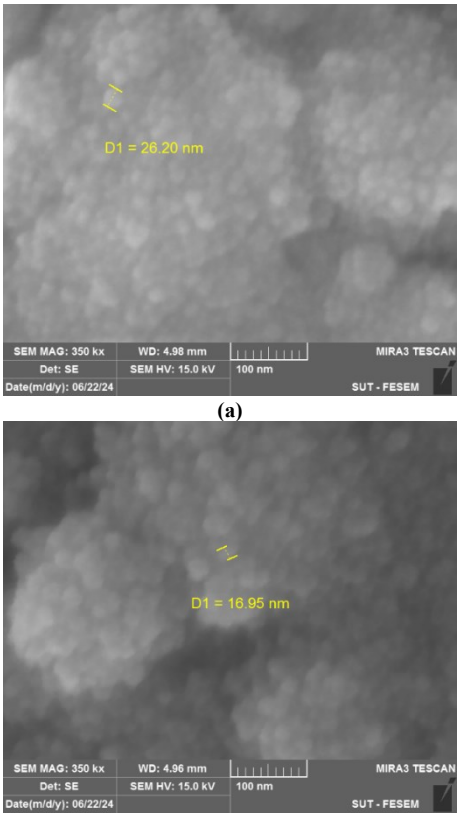

Fig. (4) SEM images for (a) ZnO 70%:SnO_2 30% and (b) ZnO 50%:SnO_2 50%

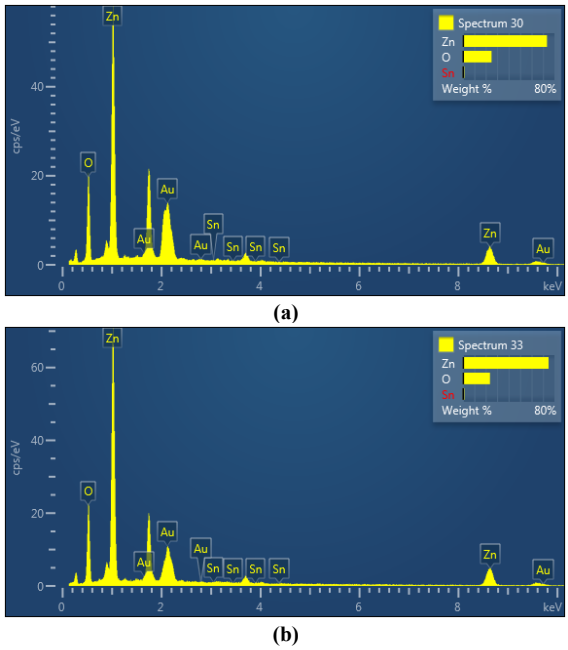

Fig. (5) EDX analysis for (a) ZnO 70%:SnO_2 30% and (b) ZnO 50%:SnO_2 50%

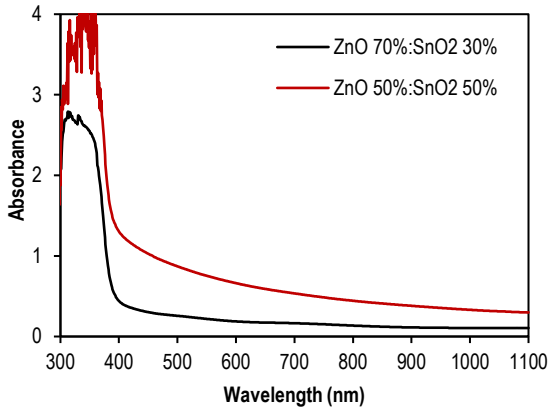

Fig. (6) Absorption spectrum for prepared samples

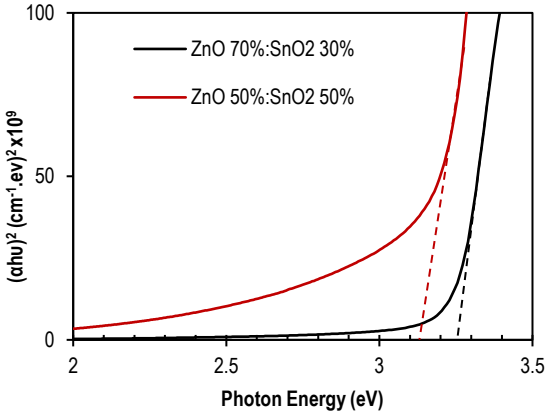

Fig. (7) Energy gap of for prepared samples

The sensitivity of the ZnO 70%:SnO_2 30% sample towards NO_2 gas was measured at 100, 150, and 200°C and showed the sensor demonstrated a reasonable improvement in sensitivity to NO_2 gas, particularly at 150°C; the sensitivity value was about 559.18%. While the sensitivity of the ZnO 50%:SnO_2 50% sample will increase significantly, reaching 1344.40% at 100°C, due to the particle size decrease resulting from the increasing doping ratio of SnO_2.

The small particle size allows a large amount of NO_2 gas particles to react with the sensor's surface. Add to that, when NO_2 gas reacts on the ZnO-SnO_2 surface, even at lower working temperatures, it absorbs electrons from physisorbed oxygen species (O_2) and becomes desorbed as NO_2 gas molecules [28, 29]. But with the temperature increased to 200°C, the films ZnO 50%:SnO_2 50% did not sense NO_2 gas; this means that the sample has become saturated, as shown in table (3).

Table (3) Sensitivity, response, and recovery time for gas sensor at different temperatures with NO_2 gas

Sample	Average Roughness (nm)	RMS Roughness (nm)	Average Grain Size (nm)
ZnO70%:SnO_2 30%	4.426	5.521	64.01
ZnO50%$SnO_2$50%	11.30	20.58	48.02

Resistance for ZnO 70%:SnO_2 30% as a function of time is displayed in Fig. (8) at 100, 150, and 200 °C; it shows resistance decreases rapidly as soon as the gas is switched on. This means that the NO_2 gas adsorption on the sensor's surface has reached saturation, whereas when the gas is stopped, resistance goes back to its starting value. But figure (9) shows resistance as a function of time when increasing the ratio of doping of SnO_2 to 50%; it shows the resistance abruptly increases until it reaches a stable condition after being exposed to gas. The sensing method is based on NO_2 chemisorption, as seen in the reaction:

NO_2 (gas) + e^- → NO_2^-

Electrons are removed from the SnO_2 surface, which increases the films resistance. The NO_2^- ions are decomposed into NO (gas) and O^- as follows:

NO_2^- → NO (g) + O^-

The O^- ions that are generated help to further raise resistance [30]. Figures (10) and (11) illustrate the response and recovery times at various ratios to the NO_2 gas of ZnO:SnO_2 gas sensors. Recovery times were longer than response times, as the sensor reacts to the gas with a low response time while taking longer to return to its original state after exposure to the gas, as shown in table (3).

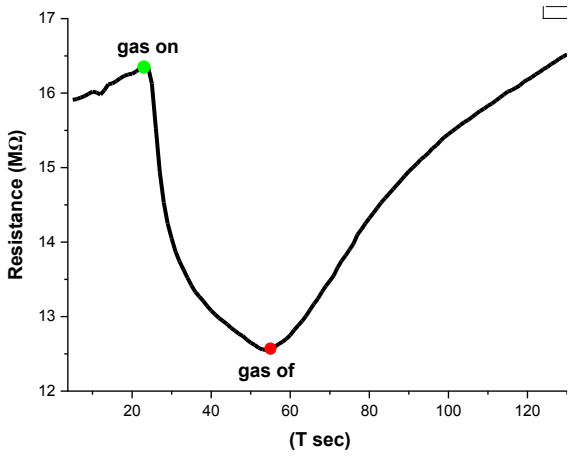

(a) 100°C

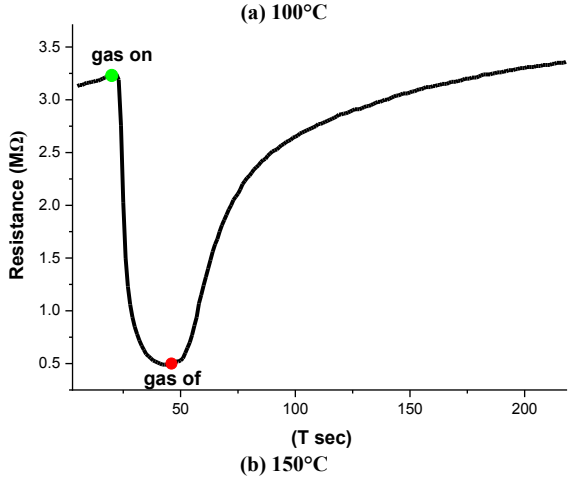

(b) 150°C

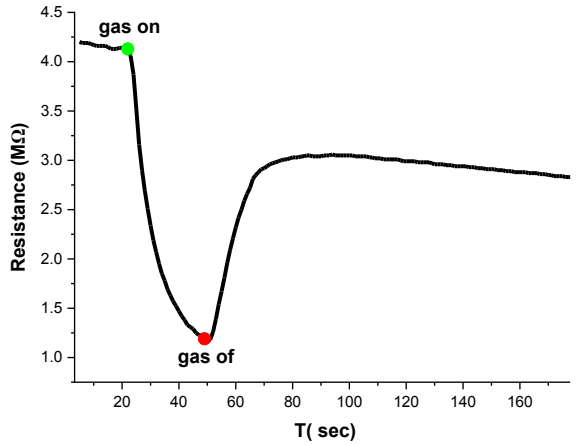

(c) 200°C

Fig. (8) Resistance as a function of time for ZnO 70%:SnO_2 30% at (a) 100°C, (b) 150°C, (c) 200°C with NO_2 gas

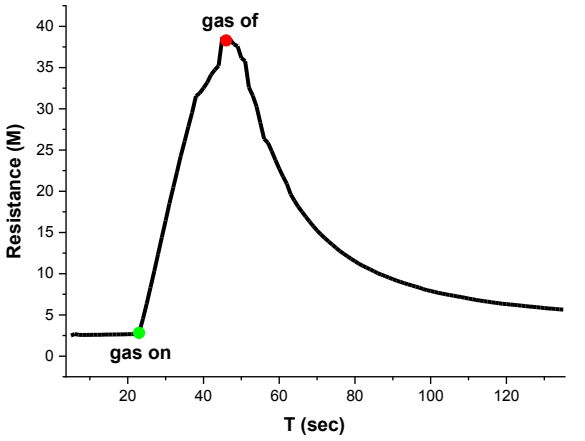

(a) 100°C

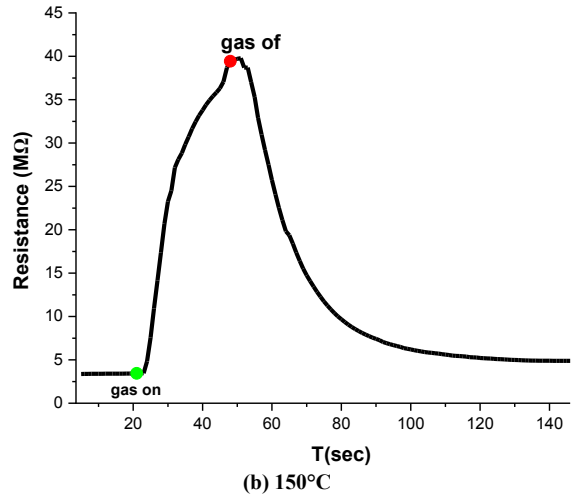

(b) 150°C

Fig. (9) Resistance as a function of time for ZnO 50%:SnO_2 50% at (a) 100°C, (b) 150°C with NO_2 gas

4. Conclusion

The ZnO:SnO_2 films show polycrystalline structure, flat surfaces with no cracks or pinholes and are homogeneous. Also, the high density of the structures and the similarity of the shapes with their repetition were confirmed. The absorption occurs in the range of about 350 nm with high absorption in the UV region, and increasing the ratio of doping of SnO_2 caused optical absorption to rise, while the optical band gap decreased from 3.22 eV to 3.05 eV. The sensitivity of ZnO films doped with different percentages of SnO_2 for NO_2 gas improved significantly as the SnO_2 doping ratio increased. The maximum sensitivity to NO_2 gas was 1344.40% for the ZnO 50%:SnO_2 50% sample at an working temperature of 100°C with a response time of 20.7 sec, while the sensitivity to the same gas was 559.18% for ZnO 70%:SnO_2 30% at a response time of 22.5 sec at 150°C.

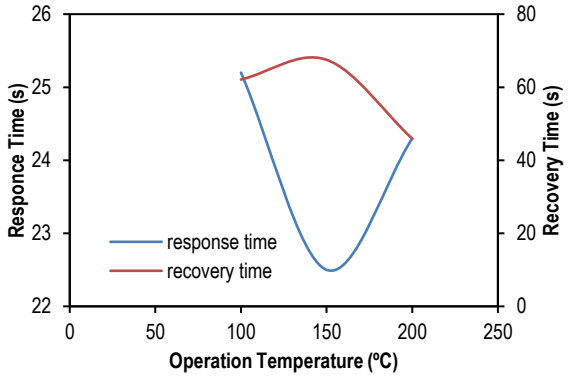

Fig. (10) The response and recovery time of ZnO 70%:SnO_2 30% as functions of operation temperature

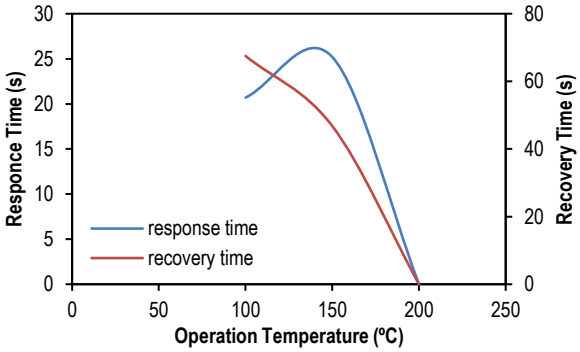

Fig. (11) The response and recovery time of ZnO 50%:SnO_2 50% as functions of operation

References

[1] Q. Li, W. Zeng and Y. Li, "Metal oxide gas sensors for detecting NO_2 in industrial exhaust gas: Recent developments", *Sens. Actuat. B: Chem.*, 359 (2022) 131579.

[2] T.H. Eom et al., "Substantially improved room temperature NO_2 sensing in 2-dimensional SnS2 nanoflowers enabled by visible light illumination", *J. Mater. Chem. A*, 9 (2021) 11168–11178.

[3] X. Li et al., "Enhanced H_2S sensing performance of $BiFeO_3$ based MEMS gas sensor with corona poling", *Sens. Actuat. B: Chem.*, 358 (2022) 131477.

[4] U. Yaqoob and M.I. Younis, "Chemical Gas Sensors: Recent Developments, Challenges, and the Potential of Machine Learning—A Review", *Sensors*, 21(8) (2021) 2877.

[5] N. Landini et al., "Nanostructured Chemoresis tive Sensors for Oncological Screening and Tumor Markers Tracking: Single Sensor Approach Applications on Human Blood and Cell Samples", *Sensors*, 20(5) (2020) 1411.
[6] A. Tricoli, M. Righettoni and A. Teleki, "Semiconductor gas sensors: dry synthesis and application", *Angew. Chem. Int. Ed.*, 49(42) (2010) 7632–7659.
[7] D.R. Miller, S.A Akbar and P.A. Morris, "Nanoscale metal oxide-based heterojunctions for gas sensing: A review", *Sens. Actuat. B: Chem.*, 204 (2014) 250–272.
[8] S.M. Sze and M.K. Lee, **"Physics of Semiconductor Devices"**, 3rd ed. John Wiley & Sons (2021).
[9] H. Wang and A.L. Rogach, "Hierarchical SnO_2 nanostructures: recent advances in design, synthesis, and applications", *Chem. Mater.*, 26(1) (2014) 123–133.
[10] A.C. Catto et al., "An easy method of preparing ozone gas sensors based on ZnO nanorods", *RSC Adv.*, 5(25) (2015) 19528–19533.
[11] G. Korotcenkov and B.K. Cho, "Ozone measuring: What can limit application of SnO_2-based conductometric gas sensors?", *Sens. Actuat. B: Chem.*, 161(1) (2012) 28–44.
[12] J. He et al., "A low-cost flexible broadband photodetector based on $SnO_2/CH_3NH_3PbI_3$ hybrid structure", *Opt. Mater.*, 88 (2019) 689–694.
[13] T.T.N. Hoa et al., "Highly selective H_2S gas sensor based on WO_3-coated SnO_2 nanowires", *Mater. Today Commun.*, 26 (2021) 102094.
[14] O. Mnethu et al., "Ultra-sensitive and selective p-xylene gas sensor at low operating temperature utilizing Zn doped CuO nanoplatelets: insignificant vestiges of oxygen vacancies", *J. Colloid Interface Sci.*, 576 (2020) 364–375.
[15] J.K. Rajput et al., "Tailoring and optimization of optical properties of CdO thin films for gas sensing applications", *Physica B: Cond. Matter*, 535 (2018) 314- 318.
[16] D. Patil. V. Patil, and P. Patil, "Highly sensitive and selective LPG sensor based on α-Fe_2O_3 nanorods", *Sens. Actuat. B: Chem.*, 152(2) (2011) 299–306.
[17] M. Bouderbala et al., "Thickness dependence of structural, electrical and optical behaviour of undoped ZnO thin films", *Physica B: Cond. Matter*, 403(18) (2008) 3326–3330.
[18] Z. Jin, T. Fukumura and M. Kawasaki, "High throuput fabrication of transition – metal doped epitaxial ZnO thin films: A series of oxide-diluted magnetic semiconductors and their properties", *Appl. Phys. Lett.*, 78(24) (2001) 3824.
[19] S. Shubra et al., "Structure , microstructure and physical properties of ZnO based materials in various forms : bulk, thin film and nano", *J. Phys. D Appl. Phys.*, 40(20) (2007) 6312–6327.
[20] P. Scherrer, Göttinger Nachrichten Gesell, Univ. zu Göttingen, 2 (1918) 98.
[21] P. Prepelita et al., "The influence of using different substrates on the structural and optical characteristics of ZnO thin films", *Appl. Surf. Sci.*, 256 (2010) 1807–1811.
[22] A.A. Hussain and Q.N. Abdullah, "Studying the Structural, Optical and Electrical Properties of ZnO:SnO_2 Thin Films as an Application of a Gas Sensor Using Vacuum Thermal Evaporation Technique", *Tikrit J. Pure Sci.*, 28(6) (2023) 66-75.
[23] D.Y. Torres et al., "Structural, morphological, optical and photocatalytic characterization of ZnO–SnO_2 thin films prepared by the sol–gel technique", *J. Photochem. Photobiol. A: Chem.*, 235 (2012) 49–55.
[24] F. Chaabouni, M. Abaab and B. Rezig, "Characterization of nZnO/p-Si films grown by magnetron sputtering", *Superlatt. Microstruct.*, 39(1) (2006) 171-178.
[25] K.S. Pakhare et al., "SILAR synthesis of SnO_2–ZnO nanocomposite sensor for selective ethanol gas", *Bull. Mater. Sci.*, 45(2) (2022) 68.
[26] Sh.M. Abed and J. Mohammed, "Preparation and characterazation of aluminum doped nanocrystalline zinc oxide for solar cells applications", *J. Ovonic Res.*, 15(1) (2019) 61-67.
[27] A.S. AlShammari et al., "Synthesis of Titanium Dioxide (TiO_2)/Reduced Graphene Oxide (rGO) thin film composite by spray pyrolysis technique and its physical properties", *Mater. Sci. Semicond. Process.*, 116 (2020) 105140.
[28] M.A. Hameed, S.H. Faisal and R.H. Turki, "Characterization of Multilayer Highly-Pure Metal Oxide Structures Prepared by DC Reactive Magnetron Sputtering Technique", *Iraqi J. Appl. Phys.*, 16(4) (2020) 25-30.
[29] A.M. Hameed and M.A. Hameed, "Highly-Pure Nanostructured Metal Oxide Multilayer Structure Prepared by DC Reactive Magnetron Sputtering Technique", *Iraqi J. Appl. Phys.*, 18(4) (2022) 9-14.
[30] L. Filipovic et al., "A Method for Simulating Spray Pyrolysis Deposition in the Level Set Framework", *Eng. Lett.*, 21(4) (2013) 224-240.

Table (1) XRD data of ZnO:SnO_2 thin films prepared at different ratios

Sample	2θ (deg)	FWHM (deg)	d_{hkl}. (Å)	G.S. (nm)	Avg G.S. (nm)	(hkl)
ZnO70%:$SnO_2$30%	31.83	0.3936	2.8119	21.0	15.48	(100)
	34.12	0.7872	2.6281	10.6		(002)
	36.33	0.4428	2.4732	18.9		(101)
	56.34	0.7872	1.6330	11.4		(220)
ZnO50%:$SnO_2$50%	31.52	0.8856	2.83864	9.3	11.78	(100)
	34.48	0.9840	2.6013	8.5		(002)
	36.43	0.8856	2.4667	9.4		(101)
	57.03	0.6888	1.6158	13.1		(220)
	61.98	0.4980	1.4322	18.6		(310)

